J. Electrochem. Sci. Eng. **13(6)** (2023) 895-909; http://dx.doi.org/10.5599/jese.2075

Open Access : : ISSN 1847-9286
www.jESE-online.org

Original scientific paper

Primary aluminum-air flow battery for high-power applications: optimization of power and self-discharge

Dayatri Bolaños-Picado[1,2], Cindy Torres[1,3] and Diego González-Flores[2,3,4,✉]

[1]*Departamento de Ingeniería Química, 11501 2060, Sabanilla de Montes de Oca, San José, Costa Rica*
[2]*Centro de Electroquímica y Energía Química (CELEQ), Universidad de Costa Rica, 11501 2060, Sabanilla de Montes de Oca, San José, Costa Rica*
[3]*Centro de Investigación en Ciencia e Ingeniería de Materiales (CICIMA), 11501 2060, Sabanilla de Montes de Oca, San José, Costa Rica*
[4]*Escuela de Química, Universidad de Costa Rica, 11501 2060, San Pedro de Montes de Oca, San José, Costa Rica*

Corresponding author: ✉*diegoandres.gonzalez@ucr.ac.cr; Tel.: +506-2511-2459*

Received: September 11, 2023; Accepted: November 2, 2023; Published: November 14, 2023

Abstract

Aluminum-air batteries are a front-runner technology in applications requiring a primary energy source. Aluminum-air flow batteries have many advantages, such as high energy density, low price, and recyclability. One of the main challenges with aluminum-air batteries is achieving high power while parasitic corrosion and self-discharge are minimized. In this study, the optimization of an aluminum-air flow cell by multiple-parameters analysis and integration of a four-cell stack are shown. We also studied the incorporation of ammonium metavanadate (NH_4VO_3) as anticorrosive in 4 mol L^{-1} KOH electrolyte by discharge and polarization plots. It was concluded that NH_4VO_3 is an efficient anticorrosive at low currents, but it limits the battery reaction at high-current and high-power applications. Nevertheless, high currents inhibit the corrosion reaction using 4 mol L^{-1} KOH electrolyte, allowing high power and capacity without anticorrosive additives. The flow in the stack also plays a significant role, and parallel flow is suggested over cascade flow since the latter results in the progressive accumulation of hydrogen as the electrolyte flows through the stack.

Keywords

Ammonium metavanadate; aluminum alloys; conversion coatings; forced flow; primary power source; backup battery

Introduction

Metal-air batteries are attractive alternatives as a power source since they have high-energy densities [1,2]. The most studied metal-air batteries include Li-air, Mg-air, Al-air, and Zn-air [3],

among which, only Zn-air batteries are rechargeable and available commercially [3,4]. Aluminum-air batteries are particularly interesting since aluminum is cheap, recyclable, and less polluting than some commercial lithium-ion batteries [5-9]. Also, aluminum is safer for the construction of batteries than other metals and has the highest volumetric energy density (8.04 Ah cm^{-3}) [3]. For that reason, some companies have even considered using primary batteries for transportation applications [10,11]. Unfortunately, in aqueous electrolytes, aluminum experiences passivation of the surface at neutral pH or corrosion at acidic or basic pH values [1]. Because of that, most reported aluminum-air batteries are primary energy sources. Nevertheless, primary batteries have a wide range of applications, such as portable devices, memory backup, hearing aids, radio, medical implants, and defense-related systems [8,9,12-14]. Typically, aluminum-air batteries with more power and capacity are flow batteries where the cell consists of an aluminum anode and an air electrode, and the electrolyte flows through the cell compartment [15-17].

As mentioned before, one of the main limitations of aluminum-air batteries is the self-corrosion of aluminum in an alkaline electrolyte, where these batteries work best. This corrosion results in self-discharge of the battery and loss of capacity. Therefore, many studies on aluminum-air batteries focus on the corrosion inhibition of the aluminum anode by forming new alloys [18-25] or utilizing some additives in the electrolyte to suppress corrosion [26-32].

Preparing new alloys typically requires complicated and expensive methodologies and costly alloying elements. On the other hand, the use of anticorrosive additives is an inexpensive methodology to improve the performance of aluminum-air batteries. Additives can be organic compounds [27,30,33-35] or inorganic salts [26,36-39]. In a prior study, we demonstrated a positive effect of ammonium metavanadate on aluminum-air batteries' performance at low current densities when using liquid-stationary or gel electrolytes [31]. Batteries with gel and liquid electrolytes with ammonium metavanadate showed higher capacities than blank samples without the additive. Moreover, batteries with liquid-stationary electrolytes showed longer operation times when ammonium metavanadate was used as an additive.

Nevertheless, most studies use batteries at very low current densities, where the anticorrosive does not have major implications for the functioning of the battery [19,40]. Aluminum-air batteries for high-power applications are rarely addressed [15,23]. As mentioned, high-power-density aluminum-air batteries require a flowing electrolyte to sustain high current densities [41,42]. Moreover, forced flow allows continuous removal of the corrosion products that inhibit the discharge of the aluminum electrode [11].

Some studies with flow batteries used dual electrolytes to avoid anode corrosion. For example, a battery with ethylene glycol and a polymeric electrolyte separated by an anionic exchange membrane was constructed, but the power density of that battery was low [43]. Some patents exist for aluminum-air flow batteries for mobility applications [11]. In that design, ultrasonic waves are used to improve the conductivity and fluidity of the electrolyte, but it is not clear how to handle aluminum corrosion. Ryu and coworkers reported one battery with higher power [44]. They developed a catalyst composed of manganese and silver and obtained power densities of more than 100 mW cm^{-2}. Current densities of 25 and 100 mA cm^{-2} were used in that study, with 6 mol L^{-1} KOH without anticorrosive additives.

In the present study, we are focused on optimizing an aluminum-air flow battery cell design and the effect of NH_4VO_3 anticorrosive on its current and power. We also integrated the optimal configuration into a four-cell stack and studied the resulting power and capacity of the battery both in parallel and in series settings.

Experimental

Reagents

Air electrode (Electric Fuel E4), Ni wire (Sigma Aldrich, 0.25 mm >99.9 %), epoxy resin (Poxipol®), KOH (Sigma-Aldrich, 99 %), NH_4VO_3 (Sigma Aldrich, >99 %), $Na_2SnO_3{\cdot}3H_2O$ (Sigma Aldrich, 95 %), and ZnO (Sigma Aldrich, >99 %).

Unit cell design

The unit cell was designed using AutoCAD 2018 modeling software. The unit cell consisted of two pieces: the cathode structure with an effective area of 5.48 cm^2 and the anodic-electrolytic structure with an effective area for the anode of 2.25 cm^2. The unit cell could contain 5.15 cm^3 of electrolyte. The unit cell was printed with ultra-high definition using a ProJet 3500 HDMax 3D printer. VisiJet M3-X polymer was used as an impression material since its mechanical properties better satisfy the chemical and mechanical requirements of the unit cell. COMSOL Multiphysics 5.5 software was used to determine the underutilized anode area.

Corrosion rate test

The annual corrosion rate of commercial aluminum alloy 5052 was determined by immersing five pieces, each with an exposed area of 5.19 cm^2, in 250 mL of treatment bath. The sampling time was every 20 min per 100 min. The solutions studied were 4 mol L^{-1} KOH, 4 mol L^{-1} KOH + 0.2 mol L^{-1} $Na_2SnO_3{\cdot}3H_2O$, 4 mol L^{-1} KOH + 0.2 mol L^{-1} NH_4VO_3, 4 mol L^{-1} KOH + 0.5 mol L^{-1} NH_4VO_3, 4 mol L^{-1} KOH + 1 mol L^{-1} NH_4VO_3, 4 mol L^{-1} KOH + 2 mol L^{-1} NH_4VO_3 and 4 mol L^{-1} KOH + 0.2 mol L^{-1} ZnO. The weight of the samples before and after immersion was measured after washing and drying the sample. The data were analyzed through the analysis of variance with the Tukey method with a significance of 0.05 using the OriginPro 8.5 software.

Anticorrosive agents

The capacity of the unit cell was determined through discharge curves using commercial aluminum alloy 5052 as an anode and a commercial air electrode as a cathode, with a PTFE membrane and an active catalytic layer of MnO_2. As electrolytes, 4 mol L^{-1} KOH, 4 mol L^{-1} KOH + 0.2 mol L^{-1} NH_4VO_3, 4 mol L^{-1} KOH + 0.5 mol L^{-1} NH_4VO_3, 4 mol L^{-1} KOH + 1 mol L^{-1} NH_4VO_3, 4 mol L^{-1} KOH + + 2 mol L^{-1} NH_4VO_3 and 4 mol L^{-1} KOH + 0.2 mol L^{-1} ZnO were used. Discharges were carried out using current densities of 0.67 mA cm^{-2} and 3.33 mA cm^{-2} with a data collection frequency of 5 s. A volumetric flow of 0.44 mL of electrolyte per second was established, supplied by a peristaltic pump. Data acquisition was performed with the EC-Lab V11.02 and Nova 2.0 software. The capacity obtained by each of the treatments was analyzed through an analysis of variance with the Tukey method with a significance of 0.05 using the OriginPro 8.5 software.

Evaluation of the anticorrosive capacity and a ventilation system

The maximum power and current density associated with this maximum were determined by measuring the voltage delivered by the unit cell with ascending current pulses at regular time intervals for each treatment. The time interval for 4 mol L^{-1} KOH treatment was 2.5 min, while for 4 mol L^{-1} KOH + 1 mol L^{-1} NH_4VO_3, it was 5 min. The sampling time was selected according to the maximum time the cell can operate before the anode has been completely consumed. For the treatments with ventilation, an airflow fan was designed in AutoCAD 2018 and printed with the same technology and material as the unit cell. Data acquisition was performed with the EC-Lab V11.02 software. A factorial design 2^2 was established, in which independent variables were

anticorrosive and a ventilation system in the unit cell. The maximum power results were analyzed through an analysis of variance with a significance of 0.05 using Minitab 19 software.

Four-cell stack assembly

The maximum power and current density associated with this maximum were determined by measuring the voltage delivered by a set of four-unit cells electrically connected in series or parallel with rising current pulses at regular time intervals of 2.5 min for each electrical setting. The total anode area was 9 cm^2. A total electrolyte recirculation system was established; the fresh electrolyte entered only the first unit cell and passed through the others until it returned to the storage tank. The volumetric flow of electrolytes was kept equal to 0.44 mL s^{-1}. Data acquisition was performed with the EC-Lab V11.02 software.

Also, through discharge curves, the operating time and the voltage capability of the four-cell stack were determined using the current density of 13.33 mA cm^{-2} when the electrical configuration was in series and 5.56 mA cm^{-2} and 11.11 mA cm^{-2} when the electrical configuration was in parallel. For both configurations, the data collection frequency was 5 s. Data acquisition was performed with Nova 2.0 software. The data were analyzed using a two-tailed Student's t-test with a significance of 0.05 using the OriginPro 8.5 software.

Results and discussion

Since the use of electric devices has been continuously increasing, more powerful and long-lasting batteries are required. Our main motivation was developing a primary aluminum-air flow battery for high-power applications. To do that, we need to reach different characteristics:

- a battery with the highest possible current density, which helps to have a compact and highly energy-dense power source,
- aluminum alloys that are cheap and commercially available,
- a battery that can have long-lasting autonomy; for that, the self-corrosion of the battery by anticorrosive additives must be suppressed.

The reactions involved in an aluminum-air battery are described by equations (1-3). The aluminum anode is oxidized, while at the cathode, oxygen is reduced. However, in an alkaline electrolyte, the aluminum anode can be spontaneously dissolved by reacting with water and forming hydrogen as a by-product, according to equation 4. This reaction is responsible for the self-discharge of aluminum-air batteries and results in mass loss of the anode and loss of capacity of the cell.

Anode: $Al + 4OH^- \rightarrow Al(OH)_4^-$ (1)

Cathode: $O_2 + 2H_2O + 4\ e^- \rightarrow 4\ OH^-$ (2)

Global reaction: $Al + O_2 + 6e^- + 4OH^- \rightarrow 4Al(OH)_4^-$ (3)

Self-corrosion: $2Al + 6H_2O + 2OH^- \rightarrow Al(OH)_4^- + H_2$ (4)

Prior studies have shown that gel electrolytes result in low current density [31], while neutral pH electrolytes usually result in low current density and low voltage. For that reason, we decided to focus on alkaline liquid electrolytes. Firstly, we prepared the unit cell design as described in Figure 1. We prepared five initial prototypes to construct our final cell prototype. One of the major issues to solve was leaking from the cell, which we solved by creating channels around the cell and using a silicon film for sealing. We also simulated the flow inside the cell using COMSOL Multiphysics. Based on those simulations, we decided to move the inlet of the electrolyte to the low end of the cell side to have a better flow and use of the surface area of the electrode (for details about it, see Supplementary material Figure S-1).

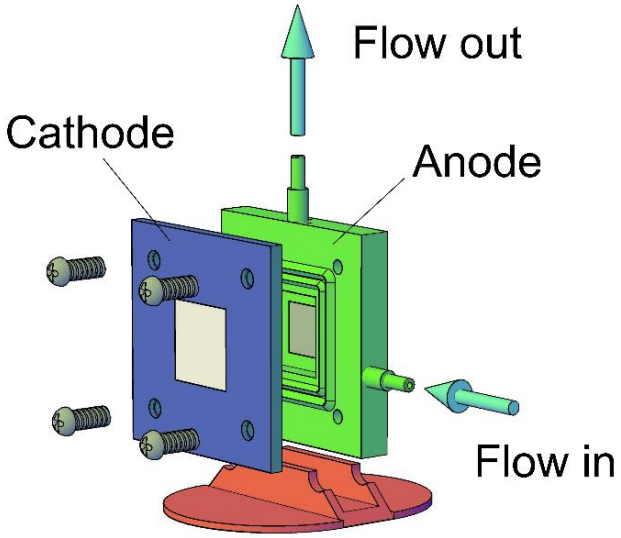

Figure 1. *Design of the unit cell (for details about the design of the unit cell design, see Supplementary material Figures S-2 and S-3)*

When we tested our cell design, we observed that the electrolyte flow was necessary for the correct functioning of the unit cell. Experiments with no electrolyte flow resulted in poor performance of the battery (see Supplementary material Table S-1). The poor performance of the unit cell could be explained by the static electrolyte promoting the accumulation of hydrogen bubbles, which decreases the conductivity of the electrolyte [45]. At the same time, the electrolyte flow helps to reduce the magnitude of polarization concentration, a well-known phenomenon that causes a decrease in the voltage delivered by the battery [45-47].

The reduction in the magnitude of the concentration polarization due to the flowing of the electrolyte is because the inherent speed of the solution movement leads to a decrease in both the thickness of the diffusion boundary layer and the difference in concentration between the surface of the electrode and the bulk solution, all due to the improvement in mass transfer. Moreover, a decrease in the concentration difference causes the value of the natural logarithm of the Nernst equation to approach unity, and therefore, the concentration polarization is decreased, improving the voltage delivered by the battery. The reduction in the ability of the electrolyte to transfer ions due to the hydrogen bubbles generated by the parasitic reaction of the system can be observed in a discharge curve as a sudden and sometimes reversible decrease in the voltage delivery, no matter if the system was provided of an anticorrosive additive or not (see Supplementary material Figures S-4 and S-5 and Table S-2).

Potassium hydroxide and sodium hydroxide solutions are usually electrolytes in metal-air batteries [17]. Potassium hydroxide was selected despite its higher cost because it has two clear advantages over sodium hydroxide. The first one is that its ionic conductivity is higher [48]. Secondly, potassium carbonate, the chemical compound that is formed due to the reaction of potassium hydroxide with the carbon dioxide of the environment, has a higher solubility than its sodic analog, which is a chemical compound that can be formed due to the reaction of sodium hydroxide with the carbon dioxide of the environment, in an aqueous environment. Generally, a greater solubility of any expected by-product in the electrolyte is desirable because it reduces the probability of clogging the channels of the active catalytic layer that allow the oxygen to get into the unit cell.

We also tested the effect of the electrolyte concentration on the performance of the unit cell, and we observed that using 4 mol L^{-1} KOH electrolyte allows working at higher current density and delivers more power than 0.1 mol L^{-1} KOH solutions (see Supplementary material Table S-2 and

Figure S-6). This is explained through the specific conductivity, which is the solution capacity to transfer ions reported for each concentration of 0.525 S cm^{-1} for the 4 mol L^{-1} KOH solution and 0.0226 S cm^{-1} for the 0.1 mol L^{-1} KOH solution [49]. High ionic conductivities are desirable as this minimizes impedance and thus improves cell operating efficiency [47]. For that reason, this electrolyte was used in further experiments. We assessed the effect of forced air in the window of the air electrode. However, there was no effect on the battery-performance (see Supplementary material Table S-3 and Figures S-7 and S-8).

It is well-known that corrosion is one of the main drawbacks of Al-air batteries. Therefore, we decided to test whether an anticorrosive additive could increase the battery performance. Using vanadates as corrosion inhibitors with sodium chloride has been widely studied [34,50,51]. However, its performance with 4 mol L^{-1} KOH and 5052 aluminum alloy in an aluminum-air flow battery was unknown until now. Considering that we have previously demonstrated the superior anticorrosive performance of ammonium metavanadate compared to zinc oxide, we decided to employ this anticorrosive in our flow battery design to optimize the required concentration of ammonium metavanadate. For that, we performed weight loss experiments. In general, in those experiments, we did not observe an appreciable anticorrosive effect for 0.2 mol L^{-1} and 0.5 mol L^{-1} solutions, but the effect became important when 1 mol L^{-1} and 2 mol L^{-1} solutions were used (see Figure 2).

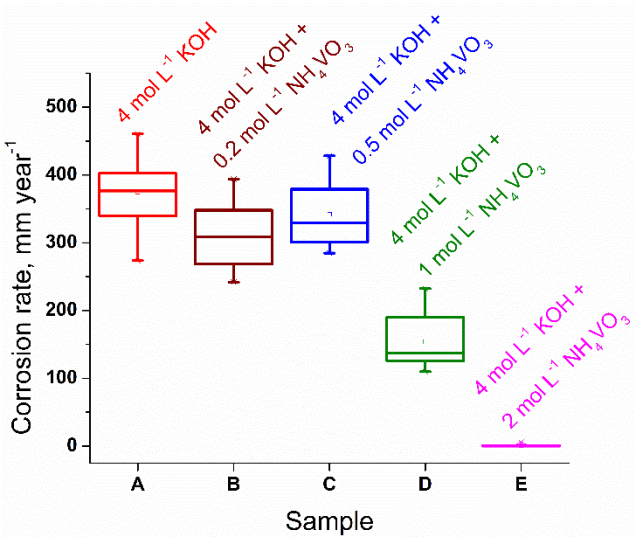

Figure 2. *Box diagram for annual corrosion rate of 5052 aluminum alloy using variable concentrations of ammonium metavanadate as anticorrosive in the electrolyte. A: 4 mol L^{-1} KOH, B: 4 mol L^{-1} KOH + 0.2 mol L^{-1} NH_4VO_3, C: 4 mol L^{-1} KOH + 0.5 mol L^{-1} NH_4VO_3, D: 4 mol L^{-1} KOH + 1 mol L^{-1} NH_4VO_3 and E: 4 mol L^{-1} KOH + 2 mol L^{-1} NH_4VO_3 (for more details see Supplementary material Figures S-9 and S-10)*

To study the effect of the anticorrosive additives on the cell performance, we decided to test the discharge plots of the black electrolyte with 4 mol L^{-1} KOH and with 0.5, 1 and 2 mol L^{-1} NH_4VO_3 (see Supplementary material Figure S-11). The discharge experiments show that (see Figure 3a) at low current density, a very superior performance of the 2 mol L^{-1} solution is obtained, that is, to the best of our knowledge, one of the highest capacities reported for this type of batteries (see Supplementary material Figure S-21). However, we observed that not all the anode material was consumed. Moreover, when we incremented the current density to 3.33 mA cm^{-2}, the same system could not sustain the current (see Supplementary material Figure S-22). In this case, the best performance of around six times that of the KOH blank solution was obtained with the 1 mol L^{-1} solution (see Figure 3b).

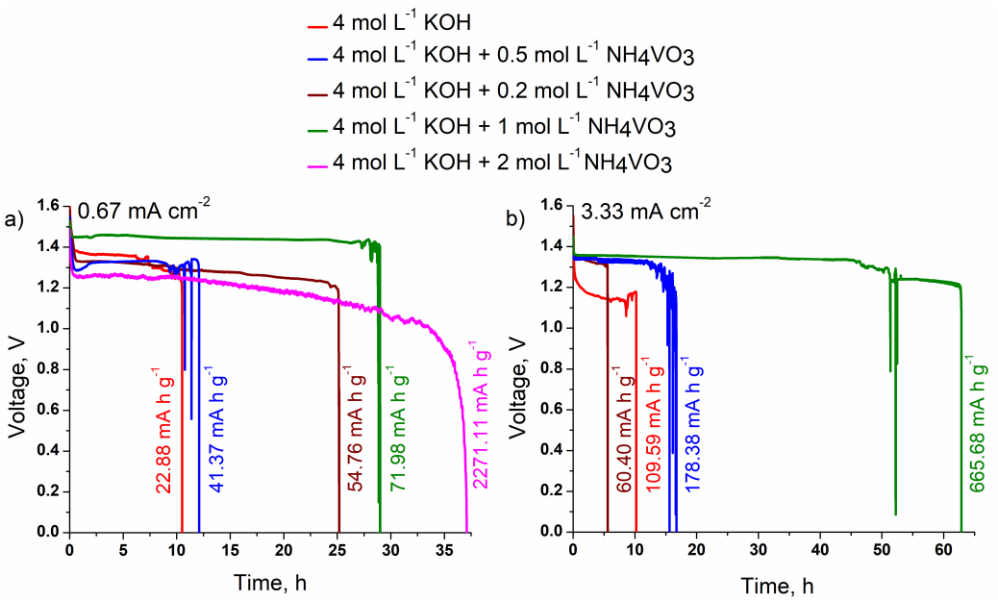

Figure 3. *Median discharge curves and capacity values obtained with the unit cell with a current density equal to a) 0.67 mA cm^{-2} and b) 3.33 mA cm^{-2}. The measurements shown correspond to the median capacity value obtained from three measurements. (For more details, see Supplementary material Table S-4 and Figures S-12 to S-20)*

As additional information and contrary to the results obtained by Wang *et al*. [52] and Liu *et al*. [30], when zinc oxide was used as an anticorrosive additive, the battery performance was inferior, regardless of current density (see Supplementary material Figures S-23-S-24). It should be taken into consideration that in the former study, they used pure aluminum and 4 mol L^{-1} KOH, while in this work, the 5052-aluminum alloy was used as an anode and 4 mol L^{-1} KOH as an electrolyte. The poor performance may be partially explained by the mechanism of how the zinc oxide protects the alloy from corrosion because it occurs by the formation of lumps on the surface of the anode, which affects the flow and is not practical, at least for its application in this flow battery (see Supplementary material Figure S-25). The lumps not only protect the anode from corrosion but also make it difficult for the desired reaction to take place, thus affecting the performance of the unit cell. Using scanning electron microscopy and X-ray energy dispersive analysis, Rashvand *et al*. [53] determined that zinc oxide produces the inhibition effect by forming a zinc-containing deposit on the aluminum surface.

In contrast, ammonium metavanadate reduces mass loss and has an adequate protection mechanism since it seemingly does not agglomerate solids on the anode surface, which may affect the voltage supply (see Supplementary material Figure S-26). According to Kharitonov *et al*. [54,55], the corrosion inhibition mechanism of vanadates is complex and involves an initial reduction of the V^{+5} species that generates V^{+4} or V^{+3} species; subsequently, oxygen in the medium enables the vanadium to return to a higher oxidation state. In this scenario of various vanadium species with different oxidation states and thanks to local acidification in the vicinity of corrosive sites, a polymeric layer of mixed valence (*i.e*., V^{+5}/V^{+4}) is formed on the surface of cathodic intermetallic particles that are part of the surface of the aluminum alloy. This polymeric layer of vanadium species is responsible for protecting the anode. In our prior study, we observed by 2D Raman imaging the formation of this polymeric species on the surface of the anode [32].

Additionally, we observed that cells presented higher capacity when potassium hydroxide batteries operated at high current density. For example, in Figure 3b, the capacity increases almost ten times when the current was increased from 0.67 to 3.33 mA cm^{-2} for samples with 1 mol L^{-1}

NH_4VO_3 additive. The same occurred for samples with pure KOH with no anticorrosive, where the capacity increased around five times with the increase in the current.

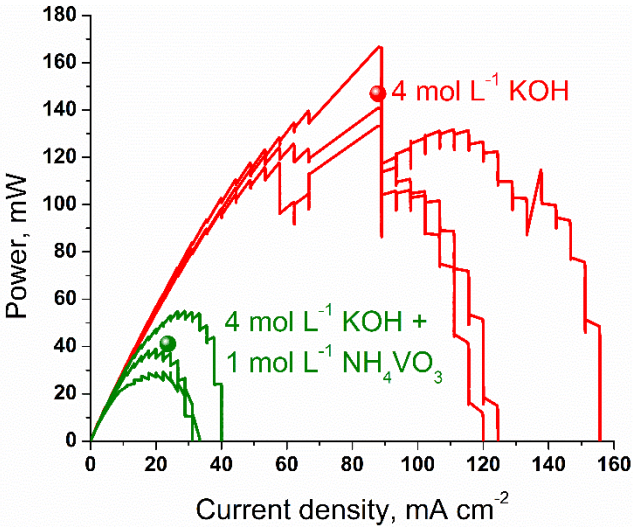

Figure 4. *Power obtained with the unit cell with and without anticorrosive in the electrolyte*

Based on those experiments, we decided to perform polarization plots to study the power of the unit cell (see Figure 4). We observed that the batteries with only potassium hydroxide could give about 4-5 times more power than those containing ammonium metavanadate. When we determined the cell power at different currents using 4 mol L^{-1} KOH (red) and 4 mol L^{-1} KOH + 1 mol L^{-1} NH_4VO_3 (green), we observed that the electrolyte without additives could give much higher power output. This means the protective polymeric layer formed by the vanadate additive lowers the corrosion and decreases the current the battery can deliver. For instance, this additive cannot be used in applications of high-power requirements.

To study the effect of the integration of cells, we decided to study the effect of connecting the batteries in series and parallel. The diagram of the connections can be seen in Figure 5. On the left figure, the connection is in series, and it is expected to obtain four times more voltage during the operation of the battery. On the other hand, the figure on the right shows the connection in parallel. In both cases, a cascade flow of the electrolyte was used.

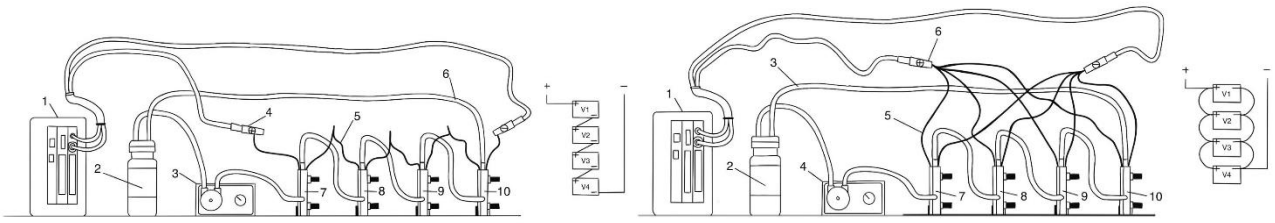

Figure 5. *Experimental diagram used in constructing discharge curves and potential jumps using a series and parallel electrical configurations*

Even though the polarization curves obtained for the unit cell indicated that the batteries with only potassium hydroxide could give more power than the batteries with ammonium metavanadate, it was decided, considering the high associated capacity, to evaluate in any case, the performance of the anticorrosive additive in the coupling of the four-unit cells. Moreover, just like when a single unit cell was evaluated, it was obtained that the power is 4 to 5 times higher when the system works without an anticorrosive additive (see Figure 6).

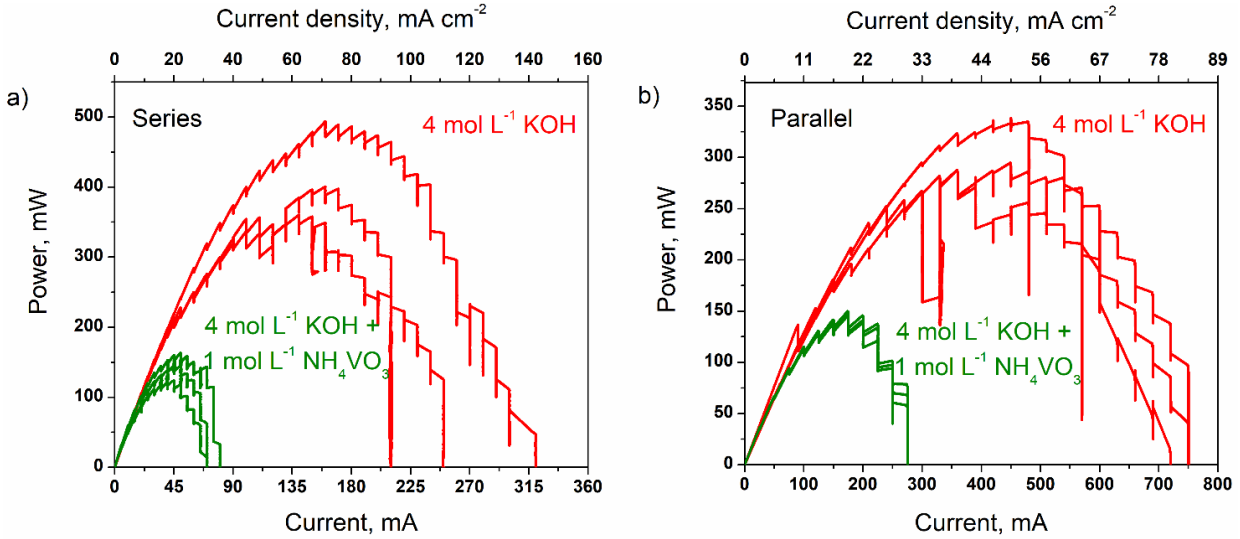

Figure 6. *Power obtained with 4-unit-cell arrangement in a) series and b) parallel electrical connection using 4 mol L^{-1} KOH (red) and 4 mol L^{-1} KOH + 1 mol L^{-1} NH_4VO_3 (green) as electrolytes. (For more details, see Supplementary material Figure S-27)*

Table 1. *Summary of performance of different battery systems*

Battery system	Maximal power, mW	Maximal voltage at maximal power, V	Maximal current at maximal power, mA
	4 mol L^{-1} KOH		
Single	166	0.84	198.07
Four in series	493	3.08	160.18
Four in parallel	338	0.75	450.15
	4 mol L^{-1} KOH + 1 mol L^{-1} NH_4VO_3		
Single	55	0.85	64.66
Four in series	163	3.27	49.98
Four in parallel	150	0.86	174.07

Table 1 shows a summary of the battery performance. For systems with 4 mol L^{-1} KOH + 1 mol L^{-1} NH_4VO_3 in series and parallel, the power was almost four times that of a unit cell. However, for systems with only 4 mol L^{-1} KOH, the obtained power was significantly lower (around 40 %) than expected compared to the power of a unit cell. Cells without additives experience losses due to the formation of hydrogen. On the other hand, cells that contain vanadate as an additive have intrinsically lower power due to the inhibition of the cell reaction by forming the protective layer over the anode.

Based on the power plots obtained, we wanted to test the four battery systems under high current-power conditions by discharge plots (see Figure 7). For the system in series, we considered the maximum current obtained in the 4 mol L^{-1} KOH + 1 mol L^{-1} NH_4VO_3 and used a slightly lower value to avoid over-demanding the battery. We have observed that it is typically difficult for the batteries to sustain the maximum power current for long periods, mainly when the anticorrosive additive is used. Therefore, we used a current at the onset of the power plot in Figure 6a, and performed discharge tests at 13.33 mA cm^{-2}. We observed that the performance was inferior for these systems with and without anticorrosive (see Figure 7a and 7b). When the batteries were operated in series, and we opened the batteries after the operation, we observed that only the first two anodes were consumed. Therefore, we conclude that one of the main reasons for this poor performance is the cascade flow of the electrolyte that accumulates hydrogen in the subsequent cell and reduces the effective area of the electrodes, resulting in less aluminum consumption in the last two cells.

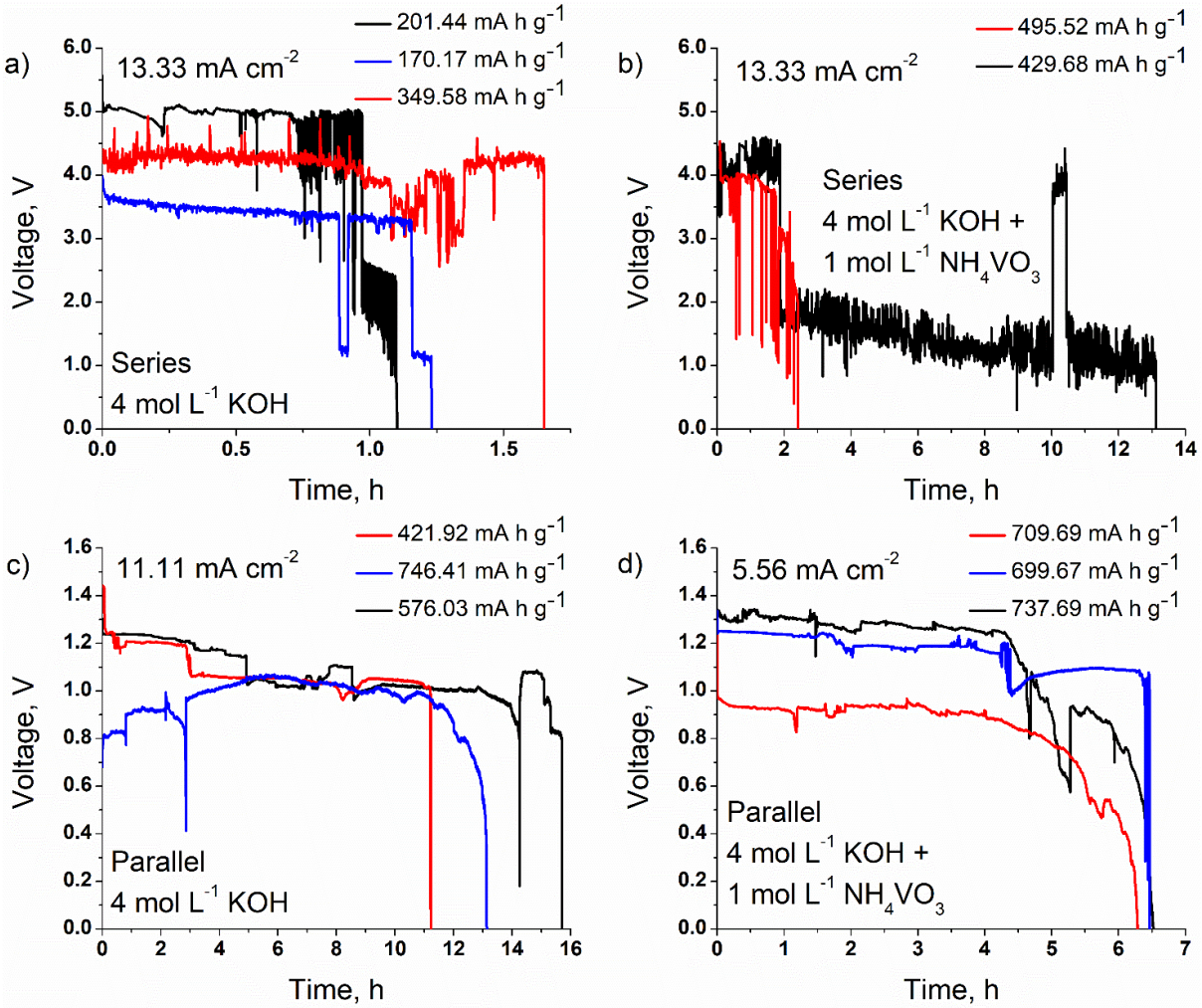

Figure 7. *Discharge curves and capacity values obtained with 4-unit cells arranged with electrical connection in series using a) 4 mol L^{-1} KOH and b) 4 mol L^{-1} KOH + 1 mol L^{-1} NH_4VO_3 with a current of 13.33 mA cm^{-2}, and with a parallel connection with c) 4 mol L^{-1} KOH at 11.11 mA cm^{-2} and with d) 4 mol L^{-1} KOH + 1 mol L^{-1} NH_4VO_3 at 5.56 mA cm^{-2}*

To test the system in parallel, we used a current density value on the onset of the power plot with 1 mol L^{-1} NH_4VO_3 (Figure 6b). For that reason, we chose 11.11 mA cm^{-2} as the discharge current. We observed that the behavior was much better for the system with 4 mol L^{-1} KOH compared to the measurements in the system in series. We also observed that the battery capacity increased significantly at this current density (see Figure 7a and 7b). On the other hand, the system with 4 mol L^{-1} KOH + 1 mol L^{-1} NH_4VO_3 could not correctly sustain the current 11.11 mA cm^{-2} in the long run (see Supplementary material Figure S-28). Therefore, we had to further decrease the current to 5.56 mA cm^{-2} to measure the discharge plots correctly (see Figure 7d). In that case, we also obtained higher capacities and better performance than the series experiments. When the system is stacked in series, its performance will be as good as the worst of the cells. Since the current has to pass through all of them, it will be limited by the cell with the most considerable resistance. When the stack is connected in parallel, the performance in the system will be the sum of all of them; therefore, it will be less susceptible to the cell with the poorest performance. For that reason, the system in parallel was more resistant and could operate for a more extended period.

From these results, we conclude that the vanadate-based additives strongly limit the current. It is more suitable for high-power applications using KOH without additives at high currents. When the

system is operated at high currents, the hydrogen formation is suppressed, and the battery can deliver more current and more capacity, even when no additive is used.

Conclusions

Ammonium metavanadate is an effective anticorrosive additive for the designed flow cell. Using 2 mol L^{-1} NH_4VO_3 in 4 mol L^{-1} KOH, one of the highest capacity values reported for liquid electrolytes is obtained [56]. However, ammonium metavanadate inhibits both the dissolution of aluminum at the open circuit and during the discharge of the battery, which limits the power the battery can deliver. This is a critical point usually not addressed in many publications about corrosion inhibitors for aluminum-air batteries. When the corrosion inhibition mechanism of an anticorrosive additive consists of blockage of the surface, it will also affect the current that the battery can deliver and its maximum power. Ammonium metavanadate is not a good fit for applications of high power. However, in low-current aluminum-air cells, it can be used as a very efficient anticorrosive additive.

Interestingly, our study shows that using high-current densities also inhibits the corrosion reaction that results in hydrogen formation, and consequently, it is possible to have higher-capacity batteries. The operation of aluminum-air batteries under high-demanding currents is an alternative for improving their efficiency and capacity. When the battery is not required, the electrolyte can be drained from the cell to avoid self-discharge by corrosion.

The flow is also an essential aspect of aluminum-air flow batteries. Since hydrogen is generated as a corrosion by-product, the accumulation of hydrogen affects the available surface area for electrochemical reactions. Therefore, cascade flow is not the best option since it accumulates hydrogen in the last cells of stacks. A parallel flow is preferable since the electrolyte enters and exits all the cells simultaneously. Also, the parallel flow typically results in fewer pressure losses through the stack.

Acknowledgements: *The authors would like to thank the funding from CONARE-FS, Posgrado en Química y Vicerrectoría de Investigación (UCR). The authors are also grateful for the support from Laboratorio Innovatio Instituto Nacional de Aprendizaje. Moreover, authors would like to thank Mario Molina and Mavis L. Montero for the fructiferous discussion.*

References

[1] T. Leisegang, F. Meutzner, M. Zschornak, W. Münchgesang, R. Schmid, T. Nestler, R. A. Eremin, A.A. Kabanov, V.A. Blatov, D.C. Meyer, The Aluminum-Ion Battery: A Sustainable and Seminal Concept?, *Frontiers in Chemistry* **7** (2019) 268. https://doi.org/10.3389/fchem.2019.00268

[2] F. Cheng, J. Chen, Metal-air batteries: From oxygen reduction electrochemistry to cathode catalysts, *Chemical Society Reviews* **41** (2012) 2172-2192. https://doi.org/10.1039/c1cs15228a

[3] Li, Qingfeng, N. J. Bjerrum, Aluminum as anode for energy storage and conversion: a review, *Journal of Power Sources* **110** (2002) 1-10. https://doi.org/10.1016/S0378-7753(01)01014-X

[4] J. S. Lee, S. T. Kim, R. Cao, N. S. Choi, M. Liu, K. T. Lee, J. Cho, Metal-air batteries with high energy density: Li-air versus Zn-air, *Advanced Energy Materials* **1** (2011) 34-50. https://doi.org/10.1002/aenm.201000010

[5] G. A. Elia, K. V. Kravchyk, M. V. Kovalenko, J. Chacón, A. Holland, R. G. A. Wills, An overview and prospective on Al and Al-ion battery technologies, *Journal of Power Sources* **481** (2021) 228870. https://doi.org/10.1016/j.jpowsour.2020.228870

[6] G. A. Elia, K. Marquardt, K. Hoeppner, S. Fantini, R. Lin, E. Knipping, W. Peters, J. F. Drillet, S. Passerini, R. Hahn, An Overview and Future Perspectives of Aluminum Batteries, *Advanced Materials* **28** (2016) 7564-7579. https://doi.org/10.1002/adma.201601357
[7] Y. Xu, Y. Zhao, J. Ren, Y. Zhang, H. Peng, An All-Solid-State Fiber-Shaped Aluminum-Air Battery with Flexibility, Stretchability, and High Electrochemical Performance, *Angewandte Chemie* **128** (2016) 8111-8114. https://doi.org/10.1002/ange.201601804
[8] Y. Wang, W. Pan, H. Y. H. Kwok, H. Zhang, X. Lu, D.Y.C. Leung, Liquid-free Al-air batteries with paper-based gel electrolyte: A green energy technology for portable electronics, *Journal of Power Sources* **437** (2019) 226896. https://doi.org/10.1016/j.jpowsour.2019.226896
[9] Y. Wang, H. Y. H. Kwok, W. Pan, Y. Zhang, H. Zhang, X. Lu, D.Y.C. Leung, Combining Al-air battery with paper-making industry, a novel type of flexible primary battery technology, *Electrochimica Acta* **319** (2019) 947-957. https://doi.org/10.1016/j.electacta.2019.07.049
[10] Y. Liu, Q. Sun, W. Li, K. R. Adair, J. Li, X. Sun, A comprehensive review on recent progress in aluminum-air batteries, *Green Energy and Environment* **2** (2017) 246-277. https://doi.org/10.1016/j.gee.2017.06.006
[11] E. Khasin, Electrolyte System for Metal-Air Batteries and Methods for Use Thereof, US 2013/0034781, 2013.
[12] J. Paniagua Rojas, J.E. González-Hernández, J. M. Cubero-Sesin, Z. Horita, D. González-Flores, Benchmarking of Aluminum Alloys Processed by High-Pressure Torsion: Al-3% Mg Alloy for High-Energy Density Al-Air Batteries, *Energy and Fuels* **37** (2023) 4632-4640. https://doi.org/10.1021/acs.energyfuels.2c03722
[13] Y. Ma, A. Sumboja, W. Zang, S. Yin, S. Wang, S. J. Pennycook, Z. Kou, Z. Liu, X. Li, J. Wang, Flexible and Wearable All-Solid-State Al-Air Battery Based on Iron Carbide Encapsulated in Electrospun Porous Carbon Nanofibers, *ACS Applied Materials & Interfaces* **11** (2019) 1988-1995. https://doi.org/10.1021/acsami.8b14840
[14] Y. Wang, H. Y. H. Kwok, W. Pan, H. Zhang, X. Lu, D. Y. C. Leung, Parametric study and optimization of a low-cost paper-based Al-air battery with corrosion inhibition ability, *Applied Energy* **251** (2019) 113342. https://doi.org/10.1016/j.apenergy.2019.113342
[15] S. Feng, G. Yang, D. Zheng, L. Wang, W. Wang, Z. Wu, F. Liu, A dual-electrolyte aluminum/air microfluidic cell with enhanced voltage, power density and electrolyte utilization via a novel composite membrane, *Journal of Power Sources* **478** (2020) 228960. https://doi.org/10.1016/j.jpowsour.2020.228960
[16] R. Buckingham, T. Asset, P. Atanassov, Aluminum-air batteries: A review of alloys, electrolytes and design, *Journal of Power Sources* **498** (2021) 229762. https://doi.org/10.1016/j.jpowsour.2021.229762
[17] R. Mori, Recent Developments for Aluminum-Air Batteries, *Electrochemical Energy Reviews* **3** (2020) 344-369. https://doi.org/10.1007/s41918-020-00065-4
[18] L. Fan, H. Lu, J. Leng, Z. Sun, C. Chen, The Study of Industrial Aluminum Alloy as Anodes for Aluminum-Air Batteries in Alkaline Electrolytes, *Journal of The Electrochemical Society* **163** (2016) A8-A12. https://doi.org/10.1149/2.0021602jes
[19] M. Pino, J. Chacón, E. Fatás, P. Ocón, Performance of commercial aluminium alloys as anodes in gelled electrolyte aluminium-air batteries, *Journal of Power Sources* **299** (2015) 195-201. https://doi.org/10.1016/j.jpowsour.2015.08.088
[20] Y. J. Cho, I. J. Park, H. J. Lee, J. G. Kim, Aluminum anode for aluminum-air battery - Part I: Influence of aluminum purity, *Journal of Power Sources* **277** (2015) 370-378. https://doi.org/10.1016/j.jpowsour.2014.12.026
[21] L. Fan, H. Lu, The effect of grain size on aluminum anodes for Al-air batteries in alkaline electrolytes, *Journal of Power Sources* **284** (2015) 409-415. https://doi.org/10.1016/j.jpowsour.2015.03.063

[22] J. Ren, J. Ma, J. Zhang, C. Fu, B. Sun, Electrochemical performance of pure Al, Al-Sn, Al-Mg and Al-Mg-Sn anodes for Al-air batteries, *Journal of Alloys and Compounds* **808** (2019) 151708. https://doi.org/10.1016/j.jallcom.2019.151708

[23] M. Nestoridi, D. Pletcher, R. J. K. Wood, S. Wang, R. L. Jones, K. R. Stokes, I. Wilcock, The study of aluminium anodes for high power density Al/air batteries with brine electrolytes, *Journal of Power Sources* **178** (2008) 445-455. https://doi.org/10.1016/j.jpowsour.2007.11.108

[24] H. Moghanni-Bavil-Olyaei, J. Arjomandi, Enhanced electrochemical performance of Al-0.9Mg-1Zn-0.1Mn-0.05Bi-0.02In fabricated from commercially pure aluminum for use. as the anode of alkaline batteries, *RSC Advances* **6** (2016) 28055-28062. https://doi.org/10.1039/c6ra02113a

[25] Q. Wang, H. Miao, Y. Xue, S. Sun, S. Li, Z. Liu, Performances of an Al-0.15 Bi-0.15 Pb-0.035 Ga alloy as an anode for Al-air batteries in neutral and alkaline electrolytes, *RSC Advances* **7** (2017) 25838-25847. https://doi.org/10.1039/c7ra02918g

[26] J. Ma, W. Li, G. Wang, Y. Xiong, Y. Li, F. Ren, Influences of L-Cysteine / Zinc Oxide Additive on the Electrochemical Behavior of Pure Aluminum in Alkaline Solution, *Journal of The Electrochemical Society* **165** (2018) 266-272. https://doi.org/10.1149/2.1071802jes

[27] C. Zhu, H. Yang, A. Wu, D. Zhang, L. Gao, T. Lin, Modified alkaline electrolyte with 8-hydroxyquinoline and ZnO complex additives to improve Al-air battery, *Journal of Power Sources* **432** (2019) 55-64. https://doi.org/10.1016/j.jpowsour.2019.05.077

[28] D. Wang, H. Li, J. Liu, D. Zhang, L. Gao, L. Tong, Evaluation of AA5052 alloy anode in alkaline electrolyte with organic rare-earth complex additives for aluminium-air batteries, *Journal of Power Sources* **293** (2015) 484-491. https://doi.org/10.1016/j.jpowsour.2015.05.104

[29] Q. X. Kang, T. Y. Zhang, X. Wang, Y. Wang, X. Y. Zhang, Effect of cerium acetate and L-glutamic acid as hybrid electrolyte additives on the performance of Al - air battery, *Journal of Power Sources* **443** (2019) 227251. https://doi.org/10.1016/j.jpowsour.2019.227251

[30] J. Liu, D. Wang, D. Zhang, L. Gao, T. Lin, Synergistic effects of carboxymethyl cellulose and ZnO as alkaline electrolyte additives for aluminium anodes with a view towards Al-air batteries, *Journal of Power Sources* **335** (2016) 1-11. https://doi.org/10.1016/j.jpowsour.2016.09.060

[31] A. P. Atencio, J. R. Aviles, M. L. Montero, D. González-Flores, P. Ocón, Performance Improvement of Alkaline-Electrolyte Aluminum-Air Batteries by NH_4VO_3-Based Additives, *Energy & Fuels* **36** (2022) 2851-2860. https://doi.org/10.1021/acs.energyfuels.1c04259

[32] A. P. Atencio, J. R. Aviles, D. Bolaños, R. Urcuyo, M. L. Montero, D. González-Flores, P. Ocón, Anticorrosive additives for alkaline electrolyte in Al-air batteries: NH_4VO_3 and polyoxometalates, *Electrochemical Science Advances* **2** (2022) e2100125. https://doi.org/10.1002/elsa.202100125

[33] Z. Moghadam, M. Shabani-Nooshabadi, M. Behpour, Electrochemical performance of aluminium alloy in strong alkaline media by urea and thiourea as inhibitor for aluminium-air batteries, *Journal of Molecular Liquids* **242** (2017) 971-978. https://doi.org/10.1016/j.molliq.2017.07.119

[34] M. Iannuzzi, G. S. Frankel, Mechanisms of corrosion inhibition of AA2024-T3 by vanadates, *Corrosion Science* **49** (2007) 2371-2391. https://doi.org/10.1016/j.corsci.2006.10.027

[35] K. Xhanari, M. Finšgar, Organic corrosion inhibitors for aluminum and its alloys in chloride and alkaline solutions: A review, *Arabian Journal of Chemistry* **12** (2019) 4646-4663. https://doi.org/10.1016/j.arabjc.2016.08.009

[36] M. W. Kendig, R. G. Buchheit, Corrosion inhibition of aluminum and aluminum alloys by soluble chromates, chromate coatings, and chromate-free coatings, *Corrosion* **59** (2003) 379-400. https://doi.org/10.5006/1.3277570

[37] G. S. Frankel, R. L. McCreery, Inhibition of Al Alloy Corrosion by Chromates, *Electrochemical Society Interface* **10** (2001) 34-38.
[38] O. Lopez-Garrity, G. S. Frankel, Corrosion inhibition of AA2024-T3 by sodium silicate, *Electrochimica Acta* **130** (2014) 9-21. https://doi.org/10.1016/j.electacta.2014.02.117
[39] R. K. Gupta, N.L. Sukiman, K. M. Fleming, M. A. Gibson, N. Birbilis, Electrochemical behavior and localized corrosion associated with Mg_2Si particles in Al and Mg alloys, *ECS Electrochemistry Letters* **1** (2012) C1-C3. https://doi.org/10.1149/2.002201eel
[40] A. A. Mohamad, Electrochemical properties of aluminum anodes in gel electrolyte-based aluminum-air batteries, *Corrosion Science* **50** (2008) 3475-3479. https://doi.org/10.1016/j.corsci.2008.09.001
[41] J. Xie, P. He, R. Zhao, J. Yang, Numerical modeling and analysis of the performance of an aluminum-air battery with alkaline electrolyte, *Processes* **8** (2020) 658 https://doi.org/10.3390/PR8060658
[42] R. Zhao, J. Xie, H. Wen, F. Wang, J. Yang, D. Zhang, Performance modeling and parameter sensitivity analyses of an aluminum-air battery with dual electrolyte structure, *Journal of Energy Storage* **32** (2020) 101696. https://doi.org/10.1016/j.est.2020.101696
[43] T. Phusittananan, W. Kao-Ian, M. T. Nguyen, T. Yonezawa, R. Pornprasertsuk, A.A. Mohamad, S. Kheawhom, Ethylene Glycol/Ethanol Anolyte for High-Capacity Alkaline Aluminum-Air Battery With Dual-Electrolyte Configuration, *Frontiers on Energy Research* **8** (2020) 189. https://doi.org/10.3389/fenrg.2020.00189
[44] J. Ryu, H. Jang, J. Park, Y. Yoo, M. Park, J. Cho, Seed-mediated atomic-scale reconstruction of silver manganate nanoplates for oxygen reduction towards high-energy aluminum-air flow batteries, *Nature Communications* **9** (2018) 3715. https://doi.org/10.1038/s41467-018-06211-3
[45] S. H. Yang, H. Knickle, Modeling the performance of an aluminum-air cell, *Journal of Power Sources* **124** (2003) 572-585. https://doi.org/10.1016/S0378-7753(03)00811-5
[46] S. Yang, W. Yang, G. Sun, H. Knickle, Secondary current density distribution analysis of an aluminum-air cell, *Journal of Power Sources* **161** (2006) 1412-1419. https://doi.org/10.1016/j.jpowsour.2006.04.143
[47] D. Linden, T. B. Reddy (Eds.), *Handbook of batteries*, McGraw-Hill, 2002. ISBN 0-07-135978-8
[48] D. M. F. Santos, C. A. C. Sequeira, J.L. Figueiredo, Hydrogen production by alkaline water electrolysis, *Quimica Nova* **36** (2013) 1176-1193. https://doi.org/10.1590/S0100-40422013000800017
[49] R. J. Gilliam, J. W. Graydon, D. W. Kirk, S. J. Thorpe, A review of specific conductivities of potassium hydroxide solutions for various concentrations and temperatures, *International Journal of Hydrogen Energy* **32** (2007) 359-364. https://doi.org/10.1016/j.ijhydene.2006.10.062
[50] M. Iannuzzi, T. Young, G. S. Frankel, Aluminum Alloy Corrosion Inhibition by Vanadates, *Journal of The Electrochemical Society* **153** (2006) B533-B541. https://doi.org/10.1149/1.2358843
[51] M. Iannuzzi, J. Kovac, G. S. Frankel, A study of the mechanisms of corrosion inhibition of AA2024-T3 by vanadates using the split cell technique, *Electrochimica Acta* **52** (2007) 4032-4042. https://doi.org/10.1016/j.electacta.2006.11.019
[52] X. Y. Wang, J. M. Wang, Q. L. Wang, H. B. Shao, J. Q. Zhang, The effects of polyethylene glycol (PEG) as an electrolyte additive on the corrosion behavior and electrochemical performances of pure aluminum in an alkaline zincate solution, *Materials and Corrosion* **62** (2011) 1149-1152. https://doi.org/10.1002/maco.201005646
[53] M. Rashvand Avei, M. Jafarian, H. Moghanni Bavil Olyaei, F. Gobal, S. M. Hosseini, M. G. Mahjani, Study of the alloying additives and alkaline zincate solution effects on the

commercial aluminum as galvanic anode for use in alkaline batteries, *Materials Chemistry and Physics* **143** (2013) 133-142. https://doi.org/10.1016/j.matchemphys.2013.08.035

[54] D. S. Kharitonov, J. Sommertune, C. Örnek, J. Ryl, I. I. Kurilo, P. M. Claesson, J. Pan, Corrosion inhibition of aluminium alloy AA6063-T5 by vanadates: Local surface chemical events elucidated by confocal Raman micro-spectroscopy, *Corrosion Science* **148** (2019) 237-250. https://doi.org/10.1016/j.corsci.2018.12.011

[55] D. S. Kharitonov, C. Örnek, P. M. Claesson, J. Sommertune, I. M. Zharskii, I. I. Kurilo, J. Pan, Corrosion Inhibition of Aluminum Alloy AA6063-T5 by Vanadates: Microstructure Characterization and Corrosion Analysis, *Journal of The Electrochemical Society* **165** (2018) C116-C126. https://doi.org/10.1149/2.0341803jes

[56] X. Li, J. Li, D. Zhang, L. Gao, J. Qu, T. Lin, Synergistic effect of 8-aminoquinoline and ZnO as hybrid additives in alkaline electrolyte for Al-air battery, *Journal of Molecular Liquids* **322** (2021) 114946. https://doi.org/10.1016/j.molliq.2020.114946